SHORT-TERM HIGH TEMPERATURE DEFORMATION AND RECOVERY IN Si_3N_4 BASED MATERIALS

JOZEF KOVALČÍK [1]*, PAVOL HVIZDOŠ[1], JÁN DUSZA[1], PAVOL ŠAJGALÍK[2], MIROSLAV HNATKO[2], MIKE REECE[3]

High temperature deformation and relaxation of two silicon nitride based materials (a reference commercial gas pressure sintered Si_3N_4 and a developed hot-pressed carbon-derived Si_3N_4/SiC nanocomposite) were investigated using quasi-static repeated loading-unloading experiments in range from 1000 to 1400 °C. This behaviour is described and evaluated in terms of a spring-dashpot model of separable elastic, visco-elastic and viscous deformation processes. The model enables to estimate the values of viscosity of the intergranular phase. The energy dissipation and then the internal friction are evaluated. The results show the significance of role played by intergranular phase that influences the deformation resistance more strongly than the microstructure. In spite of its much finer microstructure, the nanocomposite exhibits higher deformation resistance than the monolithic silicon nitride.

K e y w o r d s: nanocomposites, grain boundaries, creep, Si_3N_4, SiC

KRÁTKODOBÁ VYSOKOTEPLOTNÁ DEFORMÁCIA A RELAXÁCIA MATERIÁLOV NA BÁZE Si_3N_4

V príspevku sme sledovali vysokoteplotné a relaxačné správanie dvoch druhov materiálov na báze Si_3N_4 (komerčne vyrábaný Si_3N_4 spekaný pod dusíkovým pretlakom a vyvíjaný žiarovo lisovaný Si_3N_4/SiC nanokompozit) použitím kvázistatického zaťažovania a odľahčovania v teplotnom intervale 1000 až 1400 °C.

Správanie materiálov sme opísali a určili viskoelastickým modelom, separovaním elastickej, anelastickej a plastickej deformácie. Tento model umožnil stanoviť hodnoty viskozity intergranulárnej fázy na hraniciach zŕn. Z viskoelastického modelu sme určili hodnoty vnútorného trenia a disipáciu energie. Výsledky poukazujú na väčší vplyv intergranulárnej fázy než mikroštruktúry na vysokoteplotnú deformačnú odolnosť materiálu.

[1] Institute of Materials Research, Slovak Academy of Sciences, Watsonova 47, 043 53 Košice, Slovak Republic
[2] Institute of Inorganic Chemistry, Slovak Academy of Sciences, Dúbravská cesta 9, 842 36 Bratislava, Slovak Republic
[3] Queen Mary, University of London, Mile End Road E1 4NS, London, Great Britain
* corresponding author, e-mail: kovalcik@imrnov.saske.sk

Napriek tomu jemnejšia štruktúra nanokompozitu vykazuje vyššiu deformačnú odolnosť než monolitický Si_3N_4.

1. Introduction

Silicon nitride based materials offer a high potential of good mechanical properties at room and elevated temperatures. These properties make them to be promising materials for manufacturing ceramics parts which work at high temperatures, e.g. turbocharger rotors, valves or heat exchangers.

The silicon nitride based materials are made by liquid phase sintering [1]. Sintering aids normally used for silicon nitride are rare-earth oxides (Y_2O_3, Yb_2O_3 etc.), Al_2O_3, and alkaline earth oxides (MgO, SrO). These combine with SiO_2 on the surface if the silicon nitride powder forms a silicate phase, which covers all grains of silicon nitride and promotes liquid-phase sintering at temperatures ranging from 1700 to 1900 °C. The high temperature behaviour of Si_3N_4 based materials is controlled by the glassy and crystalline phase, which softens at lower temperature than silicon nitride grains. Deformation occurs by deformation of the bonding phase or by the transport of silicon nitride through the bonding phase. Hence, the refractoriness under load of the bonding phase plays dominant role in the high temperatures behaviour.

The best way to improve high temperature resistance of silicon nitride is to increase the apparent viscosity of the intergranular phase, which means controlling the composition and purity of the sintering aids or presence of SiC inclusion at the grain boundary [2].

A successful design of these materials requires an extensive study of their deformation and fracture characteristic at temperature similar to the working ones. Although a large amount of work has been done on all these problems, still data of internal friction is required, and little is known about the values of viscosity of the intergranular glassy phases.

Conventionally used creep tests in compression, bending and tensile mode require a large number of specimens as well as long-time testing periods [3–6]. Moreover, they do not reflect the cyclical character of load experienced by ceramic parts in practice. Some authors [7, 8] elaborated a method of short-term creep tests with the aim to simplify the high temperature testing procedure. Using the model of deformation suggested in the mentioned papers, a simple method for describing deformation and relaxation behaviour has been developed [9–11]. This method, used together with SEM and TEM observation of the material before and after mechanical testing, provides an easy way to distinguish different deformation and damage mechanisms during the test.

While quantitative information achieved by using long-term bending, or rather tensile creep tests are indispensable in ceramic components design, for material

development the data obtained using time and consuming methods can be very beneficial.

The aim of the present work is to estimate high-temperature elastic moduli, internal friction, and viscosity of the intergranular glassy phases of a standard industrial silicon nitride and carbon-derived Si_3N_4/SiC nanocomposite in temperature range from 1000 to 1400 ℃ using short-time deformation behaviour study.

2. Experimental material and procedure

The materials used in this investigation were monolithic ESIS Si_3N_4 (a commercial reference silicon nitride SL200 [12, 13]) and carbon derived (CD) Si_3N_4/SiC nanocomposite.

The monolithic ESIS silicon nitride was fabricated by CeramTech, Plochingen, Germany. It is a gas pressure sintered silicon nitride with additives Al_2O_3 (3 wt.%) and Y_2O_3 (3 wt.%). The material is provided by the manufacturer in form of plates with dimensions of 47 × 11 × 102 mm^3. The CD nanocomposite was prepared at the Institute of Inorganic Chemistry of the Slovak Academy of Sciences in Bratislava by the following preparation method: The starting mixture (83.12 wt.% Si_3N_4, 4.43 wt.% Y_2O_3, 7.39 wt.% SiO, 4.05 wt.% C) was homogenized in a polyethylene bottle with Si_3N_4 spheres by attrition in isopropanol for 4 h. The subsequently dried mixture was sieved through 25 μm sieve in order to eliminate large hard agglomerates. The green discs were pressed under 25 MPa and then were embedded into BN hexagonal powder bed and positioned into a graphite uniaxial die. The samples were hot-pressed under a specific heating regime, atmosphere and mechanical pressure at 1750 ℃ for 2 h. Finished specimens had the shape of disc with the diameter of 50 mm and thickness of 5 mm.

The microstructure of the material was observed on the cut, polished and etched samples (plasma and/or chemically etched), using optical and scanning electron microscopy.

Specimens of the both materials with dimensions 3 × 4 × 45 mm^3 were cut from the sintered plates and their surface was ground by diamond wheels and polished by diamond paste to 1 μm finish.

The high temperature deformation and fracture behaviour were evaluated by four-point bending test utilizing 40/20 mm span in the creep furnace with a dead weight loading system in ambient air. The specimens deflection, between its center and the inner rollers, was measured by two inductive transducers and the data were collected by a computer controlled data acquisition system with the accuracy of about 2 μm. The load-displacement data were converted to the outer fiber stress and strain using the standard procedure [14]. Specimens were loaded by a dead weight in the temperature range from 1000 to 1400 ℃ and held in a static mode at the specified temperatures for 5 minutes. After unloading the specimens were held at the same temperature for another 10 minutes to record the relaxation

process. The relative deformation and relaxation at different temperatures as a function of time was recorded. A low residual load ($\sim$ 10 MPa) remained on each specimen after unloading to maintain the integrity of the loading system. The loading/unloading was repeated several times to simulate a cyclical test with a rectangular load waveform.

Hsueh [15] proposed a method of calculating the viscosity and two elastic moduli by analyzing a combined experiment consisting of a deformation with a constant strain rate followed by stress relaxation at zero strain rate. However, in applying this method only three individual values of the whole curve are used, which means that the greater part of the obtained information is neglected. Also, it would be more difficult to adapt our loading system for this technique. In our work Maxwell spring-dashpot model was chosen to describe creep and strain relaxation behaviour [10, 11, 15]. The model effectively represents the high temperature deformation/relaxation, and with certain simplification offers a simple way how to separate elastic, anelastic and plastic parts of it. The model used in this study is illustrated in Fig. 1. The mechanical model contains two spring and two dashpot elements in three segments designated as 1, 2, and 3. In this model, the stretching of the spring segment 1 represents elastic deformation, the stretching of the segment 2 (combination of a spring and a dashpot in parallel) the viscoelastic deformation, and the displacement of the dashpot segment 3 represents the viscous flow. The total deformation resulting from the application stress σ_o for time t is the sum of the elastic, viscoelastic and viscous deformations of applicable segments, and is given by

$$\varepsilon = \frac{\sigma_\mathrm{o}}{E_1} + \frac{\sigma_\mathrm{o}\left(1 - \mathrm{e}^{-t/\tau}\right)}{E_2} + \frac{(\sigma_\mathrm{o} t)}{\eta_3}, \tag{1}$$

where ε is total strain, σ_o is the applied stress, τ is the relaxation time given by η_2/E_2. The constants representing the resistance to elastic stretching and viscous flow, respectively, are the elastic moduli E_1, E_2, and viscosities η_2 and η_3, respectively. The subscripts indicate the segment designation. The details of the model are described in [11]. The model is valid for "short-term" creep behaviour, by which the primary creep stage and the subsequent "pseudo" steady-state stage is understood. Assuming this, the viscous part can be approximated by a straight line and Eq. (1) can be used.

From the calculated stress-strain loops the dissipated energy, and thus the internal friction, was estimated for each temperature. Internal friction is characterized by a relative amount of energy dissipated in one cycle, ψ, which is ratio of ΔW (energy dissipated in one cycle – anelastic energy), and the total recoverable strain energy, W, stored by the system in one cycle

$$\psi = \Delta W/W = \varepsilon_\mathrm{A}\sigma/(\varepsilon_\mathrm{E}\sigma/2 + \varepsilon_\mathrm{A}\sigma) = 2\varepsilon_\mathrm{A}/(\varepsilon_\mathrm{E} + 2\varepsilon_\mathrm{A}), \tag{2}$$

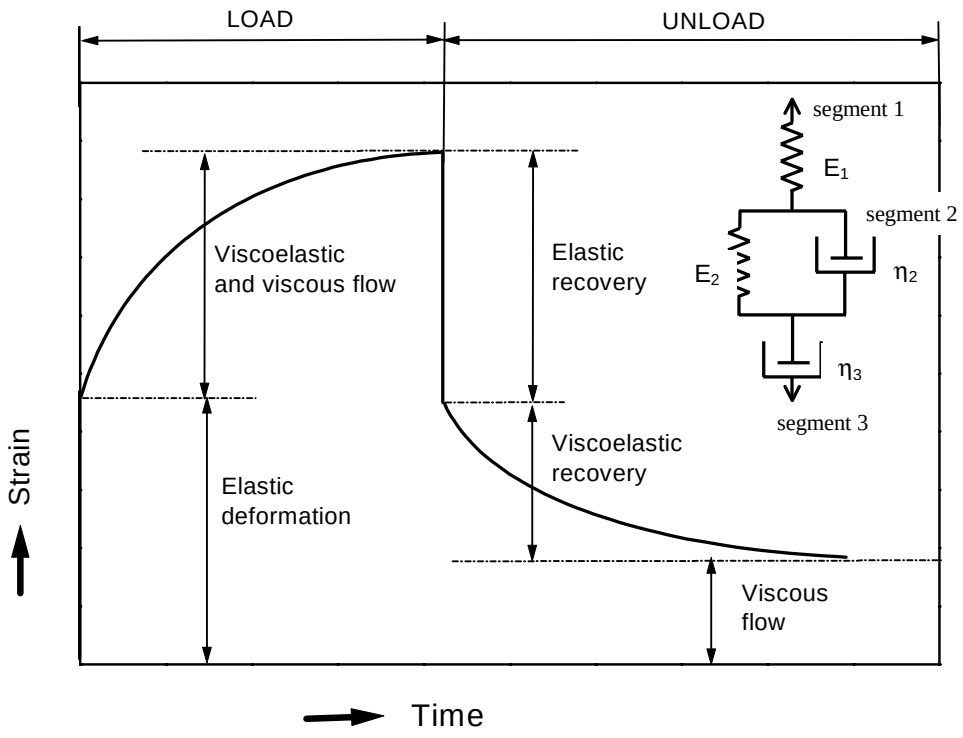

Fig. 1. Spring-dashpot model of the global high temperature behaviour.

where ε_{E} and ε_{A} are the elastic and anelastic parts of strain, respectively.

3. Results and discussion

The microstructure of the ESIS Si_3N_4 material illustrated in Fig. 2 shows moderately elongated Si_3N_4 grains with the aspect ratio of approximately three. The grains were bound together with an amorphous phase. Some microporosity and some iron containing inclusion could be recognized.

The microstructure of the carbon-derived Si_3N_4/SiC material is shown in Fig. 3. It consists of hexagonal β-Si_3N_4 grains, SiC nanoparticles and intergranular phase. Volume fraction of Si_3N_4 grains obtained by automatic analysis was 70.8 %, the intergranular phase 26 %, and that of intragranulary located nanoparticles SiC was 3.2 %. The nanoparticles located on the interface boundary are difficult to identify, so their volume fraction is included into volume fraction of intergranular phases.

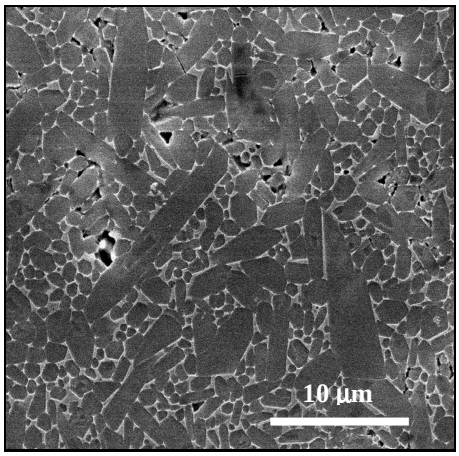

Fig. 2. Characteristic microstructure of the ESIS Si_3N_4, plasma etched, SEM.

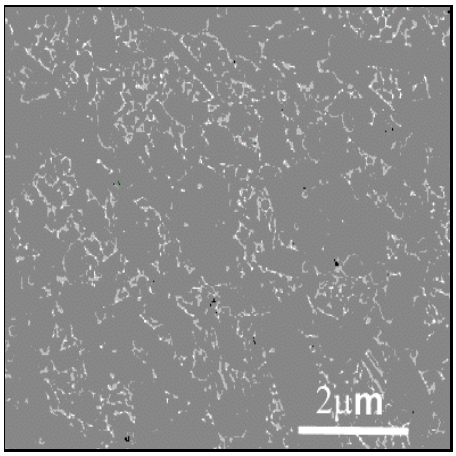

Fig. 3. Characteristic microstructure of the carbon-derived Si_3N_4/SiC nanocomposite, plasma etched, SEM.

The performance experiments have shown that below the temperature 1200 ℃ no or only very small viscous deformation but some viscoelastic recovery was detected at all applied stresses in both studied materials. Above the temperature of 1200 ℃ the materials exhibited higher viscoelastic strain recovery and viscous deformation independent of total accumulated strain. The deformation/relaxation behaviour of the ESIS Si_3N_4 is illustrated in Fig. 4 in strain-time representation at 100 MPa. At 1400 ℃ the fracture was not immediate and it was possible to evaluate parameters of the elastic and approximately also those of the viscoelastic deformation. The deformation/relaxation behaviour of the carbon derived Si_3N_4/SiC is illustrated in Fig. 5 in strain-time representation at 100 MPa. At the same conditions the ESIS material had more intensive viscoelastic and viscous deformation than the nanocomposite. A comparison of the deformation/relaxation behaviour of the experimental materials at 1200 ℃ and 200 MPa is shown in Fig. 6. At higher temperatures the differences were, generally, even greater.

From deformation/relaxation behaviour in the strain-time plots at each temperature and applied stress, the components of deformation were separated, and the effective moduli of elasticity, strain rates, characteristic times, viscosities, and internal friction were calculated from Eqs. (1) and (2). The results are shown in Table 1.

With the increased temperature the values of effective elastic modulus and viscosity decreased in both studied materials. In the whole experimental temperature interval the values were systematically lower for the monolithic Si_3N_4 than for

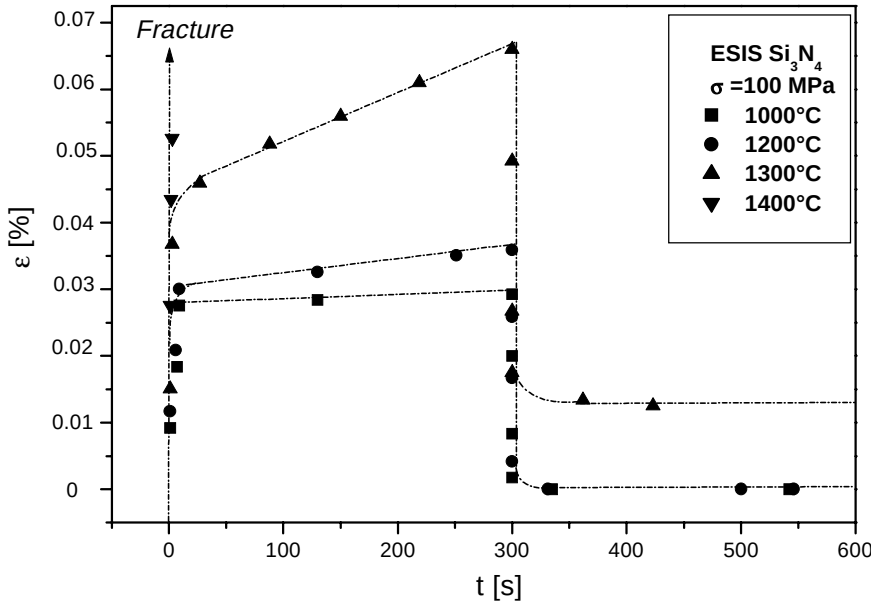

Fig. 4. Deformation/relaxation behaviour of the ESIS Si_3N_4 in strain-time representation at 100 MPa.

T a b l e 1. Calculated effective moduli of elasticity, viscosity and internal friction

Material	T [℃]	E_1 [GPa]	η_2 [Pa·s]	η_3 [Pa·s]	ψ
ESIS	1000	334±22	$2.32\times10^{14}\pm5.07\times10^{13}$	$4.99\times10^{14}\pm2.17\times10^{14}$	0.10±0.02
Si_3N_4	1200	305±9	$9.26\times10^{13}\pm4.54\times10^{13}$	$4.75\times10^{14}\pm1.5\times10^{14}$	0.14±0.03
	1300	169±114	$5.14\times10^{13}\pm2.69\times10^{13}$	$3.64\times10^{13}\pm2.79\times10^{13}$	0.17±0.04
	1400	175±55	1.49×10^{13}	$1.52\times10^{12}\pm1.09\times10^{12}$	0.30
Carbon-	1000	495±35	$2.02\times10^{14}\pm8.35\times10^{13}$	$1.52\times10^{15}\pm1.03\times10^{15}$	0.17±0.06
derived	1200	384±40	$1.49\times10^{14}\pm6.59\times10^{13}$	$6.18\times10^{14}\pm2.14\times10^{14}$	0.14±0.02
Si_3N_4	1300	354±28	$7.86\times10^{13}\pm1.86\times10^{13}$	$2.63\times10^{14}\pm3.01\times10^{13}$	0.25±0.04
/SiC	1400	320±18	$4.52\times10^{13}\pm1.05\times10^{13}$	$8.2\times10^{13}\pm1.39\times10^{13}$	0.35±0.05

the nanocomposite, which shows the positive effect of SiC on the high temperature deformation resistance. The measured values of elastic moduli corresponded fairly well with literature data (E = 310 GPa for high density HPSN), although they seem to be systematically slightly overestimated. Nevertheless, their mutual comparison remains valid. In both materials internal friction increased as the viscosity decreased with temperature, and the materials were able to comply and then to

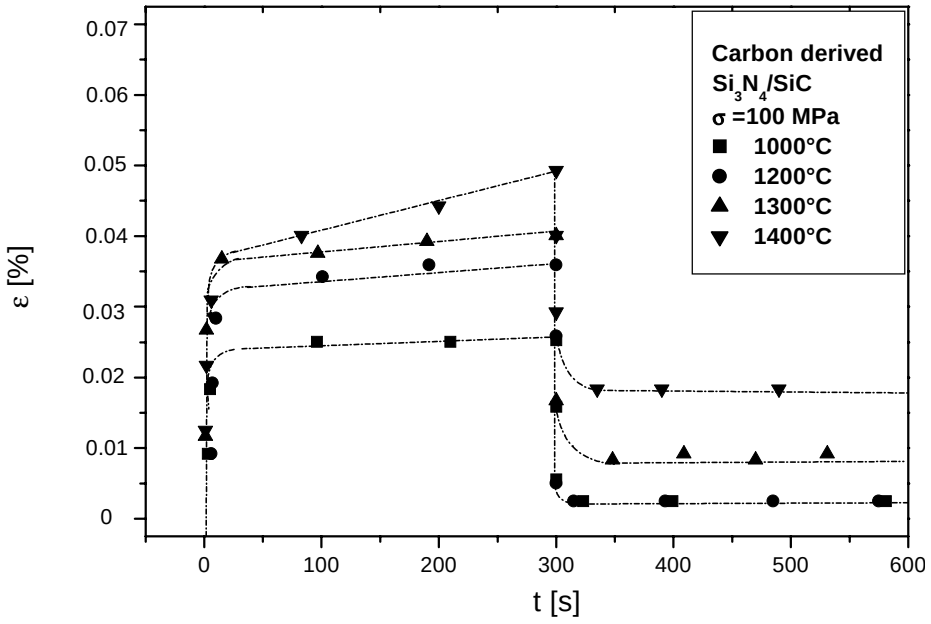

Fig. 5. Deformation/relaxation behaviour of the carbon-derived Si_3N_4/SiC nanocomposite in strain-time representation at 100 MPa.

relax in greater extent. The internal friction of the carbon-derived Si_3N_4/SiC was slightly higher than that of the ESIS Si_3N_4 material. This was probably caused by finer microstructure of the CD nanocomposite, which enables easier rotation of smaller matrix grains. Fig. 7 shows the change of viscosity with temperature for ESIS and CD. Above 1200 ℃ the viscosity of ESIS is much lower than that of CD because SiC nanoparticles present in the composite are responsible for the increase of the grain boundary phase rigidity. The characteristic times, expressing the rate of viscoelastic deformation/recovery were generally similar in the range from 20 s to 60 s for both materials. Assuming that viscous flow of the intergranular glassy phase is the easiest mechanism of deformation, which acts faster and takes place at lower temperatures than diffusion and/or dislocation movement within the matrix Si_3N_4 grains, one can deduce that the viscosity η_2 of the Maxwell element essentially corresponds to the apparent viscosity of the intergranular phase. The values of viscosity obtained from our results were a couple of orders of magnitude higher than that found by other methods for bulk silicate glass ($7.9 \times 10^{12} - 1 \times 10^9$ Pa·s at 1100–1400 ℃ [16] measured by isothermal deformation) or for grain boundary glassy layers in hot-pressed Si_3N_4 (10^{14} Pa·s at 900 ℃ [18]) and Si_3N_4/SiC ($2.5 \times$ $\times 10^8$ Pa·s at 1500 ℃ [18]), the two latter measured by a torsional pendulum. This

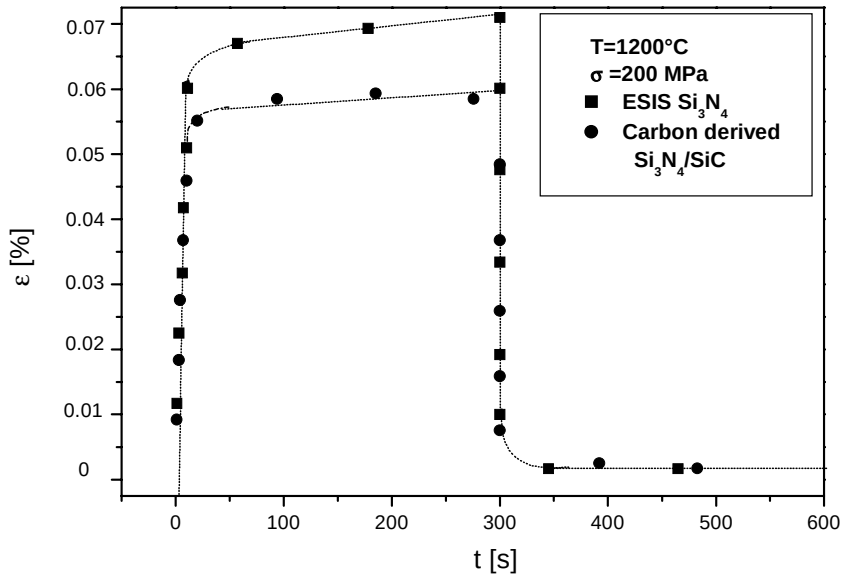

Fig. 6. Comparison of the deformation/relaxation of the studied materials at 1200 °C and 200 MPa.

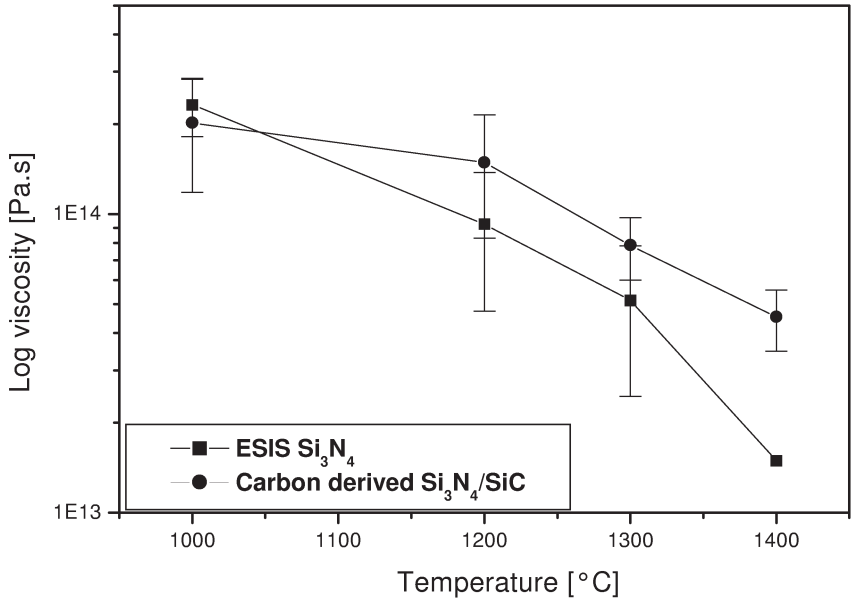

Fig. 7. Change of viscosity η_2 of the studied materials with temperature.

may be partly due to shorter time of our experiments and also by the composition and thinness of the intergranular phase, which particularly in the case of the nanocomposite proved to be highly creep resistant. However, the macroscopic viscosity of the polycrystal (η_3) calculated from the permanent strain, accumulated during the test in the sample, is in a good agreement with the values found by Pezzotti and Ota (10^{13} Pa·s for $\varepsilon_p \sim 10^{-4}$ [19, 20]).

The higher viscosity for the CD nanocomposite than for the monolithic material correlates well with its generally higher rigidity and better creep resistance. This trend is also confirmed by the minimum strain rates which are shown in the Table 2 for all experimental temperature/stress conditions.

Table 2. Calculated strain rate for the ESIS Si_3N_4 and carbon derived Si_3N_4/SiC

T [°C]	Stress [MPa]	$\dot{\varepsilon}$ [s^{-1}], ESIS Si_3N_4	$\dot{\varepsilon}$ [s^{-1}], Carbon derived Si_3N_4/SIC
1000	50	–	–
	100	5.9×10^{-8}	1.34×10^{-8}
	150	8.46×10^{-8}	8.26×10^{-8}
	200	1.65×10^{-7}	9.17×10^{-8}
	250	2.07×10^{-7}	1.09×10^{-7}
1200	50	2.84×10^{-8}	4.58×10^{-8}
	100	6.9×10^{-8}	6.26×10^{-8}
	150	1.38×10^{-7}	9.17×10^{-8}
	200	1.72×10^{-7}	9.22×10^{-8}
	250	2.76×10^{-7}	3.12×0^{-7}
1300	50	3.69×10^{-7}	–
	100	7.2×10^{-7}	1.46×10^{-7}
	150	9.2×10^{-7}	2.6×10^{-7}
	200	1.35×10^{-5}	2.7×10^{-7}
	250	–	3.27×10^{-7}
1400	50	7.04×10^{-6}	–
	100	5.13×10^{-5}	4.72×10^{-7}
	150	–	6.88×10^{-7}
	200	–	9.68×10^{-7}
	250	–	1.47×10^{-6}

4. Conclusions

A simple and fast testing procedure was used for characterizing the short-term deformation and relaxation behaviour of an industrial reference silicon nitride and

a newly developed carbon-derived Si_3N_4/SiC nanocomposite. The main results can be summarized:

– clear differences in the deformation/relaxation behaviour between the studied materials were observed,

– the influence of the intergranular phase on the deformation resistance was stronger than that of microstructural parameters (matrix grain size and shape),

– the CD nanocomposite showed much higher creep resistance and rigidity (higher effective elastic modulus, higher apparent viscosity) while exhibiting slightly higher internal friction due to the finer microstructure.

Acknowledgements

The work was supported by NANOSMART, Centre of Excellence, SAS, and financed by the Slovak Grant Agency for Science via grant No. 2/1166/21.

REFERENCES

[1] WIEDERHORN, S. M.: Z. Metallkd., *90,* 1999, p. 1053.
[2] ŠAJGALÍK, P.—HNATKO, M.—LENČÉŠ, Z.—DUSZA, J.: Key Engineering Materials, *233*, 2002, p. 201.
[3] BECHER, P. F.: J. Amer. Ceram. Soc., *74*, 1991, p. 255.
[4] WIDERHORN, S. M.—FULLER, E. R.: Mater. Sci. and Eng., *71*, 1985, p. 169.
[5] CANNON, W. R.—LANGDON, T. G.: J. Mater. Sci., *18*, 1983, p. 1.
[6] FETT, T.—MUNZ, D.: Int. J. High Tech. Ceram., *4,* 1988, p. 281.
[7] GORING, J.—BRAUE, W.—KLEEBE, H. J.: Key. Engineering Materials, *89-91*, 1994, p. 641.
[8] GU, W.—PORTER, J. R.—LANGDON, T. C.: J. Am. Ceram. Soc., *77*, 1994, p. 1679.
[9] WOODFORD, D. A.: J. Am. Ceram Soc., *81*, 1998, p. 2327.
[10] HVIZDOŠ, P.—DUSZA, J.—RUDNAYOVÁ, E.: In: Proc. of 4th Europ. Ceram. Soc. Conf. Eds.: Meriani, S., Sergo, V. Vol. 3. Riccione 1995, p. 205.
[11] HVIZDOŠ, P.: In: Fracture Mechanics of Ceramics. Eds.: Bradt, R. C., Munz, D., Sakai, M., Shevchenko, V., White, K. Vol. 13. New York – Boston – Dordrecht – London – Moscow, Kluwer Academic/Plenum Publishers 2002, p. 335.
[12] LUBE, T.—DANZER, R.: In: Fracture mechanics beyond 2000. Eds.: Neimitz, A. Rokach, I. V., Kocanda, D., Golos, K. p. 401.
[13] LUBE, T.—DANZER, R.—KUBLER, J.—DUSZA, J.—ERAUW, J.-P.—KLEMM, H.—SGLAVO, V. M.: In: Fracture mechanics beyond 2000. Eds.: Neimitz, A., Rokach, I. V., Kocanda, D., Golos, K. p. 409.
[14] HOLLENBERG, G.—TERWILLIGER, G. R.—GORDON, R. S.: J. Am. Ceram. Soc., *54*, 1971, p. 196.
[15] HSUEH, C.–H.: J. Am. Ceram. Soc., *69*, 1986, C-48–49.
[16] PEREZ, J.: Acta Metall., *32*, 1984, p. 2163.
[17] URBAIN, G.—BOTTINGA, Y.—RICHET, P.: Geochimica et Cosmochimica Acta, *46*, 1982, p. 1061.
[18] MOSHER, D. R.—RAJ, R.—KOSSOWSKY, R.: J. Mat. Sci., *11*, 1976, p. 49.
[19] PEZZOTTI, G.—OTA, K.—KLEEBE, H. J.—OKAMOTO, Y.—NISHIDA, Y.: Acta Metall. Mater., *43*, 1995, p. 4357.

[20] PEZZOTTI, G.—OTA, K.: J. Jpn. Ceram. Soc., *105*, 1997, p. 1.

Received: 27.5.2003
Revised: 22.7.2003